

Packing and percolation of poly-disperse discs and spheres

Takashi Odagaki, Tsuyoshi Okubo, Ryusei Ogata,*
and Keiji Okazaki†

Department of Physics, Kyushu University, Fukuoka 812-8581 Japan

† Mitsubishi Chemical Corporation,
Science and Technology Research Center, Yokkaichi 510-8530 Japan

November 20, 2018

Abstract

Random dense packing of poly-disperse discs and spheres generated under the infinitesimal gravity protocol is investigated by a Monte Carlo simulation. For the binary discs packed in two dimensions, the packing fraction of disc assembly becomes lower than that of the monodisperse system when the size ratio is close to unity. We show that the suppressed packing fraction is caused by an increase of the adjacent neighbours with long bonds where the adjacent neighbours is defined on the basis of the Laguerre (radical) tessellation.

For the poly-disperse systems in two and three dimensions, the packing fraction is shown to have a minimum as a function of the poly-dispersity. Percolation process in the densely packed discs and spheres is also studied. The critical area (volume) fraction in two (three) dimensions is shown to be a monotonically increasing (decreasing) function of the poly-dispersity.

1 Introduction

Random close packing of spheres is an important concept in understanding the structure and properties of liquids and glasses. The first significant contribution in this direction was reported by Bernal[1] who analyzed the structure of glasses on the basis of the sphere packing. It is also well known that solidification of liquids[2] and the flow of granular materials[3] are closely related to packing properties of hard spheres.

In practical applications, it is common to encounter systems in which the size of dispersed particles is not unique but has a certain distribution. For example, a functional composite system can be fabricated by depositing nano-clusters which are synthesized by the plasma-gas-condensation technique. In this case, the size distribution of the nano-clusters plays important role in determining the properties of the composite system[4]. Beside the packing fraction, the connectivity of particles is also important

*Present address: NEC Corporation, Tokyo, Japan

characteristics of the system composed with dispersed spheres. For example, a printing ink consists of carbon blacks dispersed in a varnish, and the network formation of carbon blacks is one of the key parameters controlling the properties of the ink. It is, therefore, important in practical applications to find out the dependence of packing fraction and connectivity on the width of the distribution or the poly-dispersity.

In this paper, we investigate the packing fraction for a random dense packing of binary hard discs and of poly-disperse hard discs and spheres. In order to avoid subtlety in the definition of random close packing[5], we study the dense packing produced by the drop-and-roll or the infinitesimal gravity protocol using a Monte Carlo simulation. Although the structure produced by this protocol is not the random close packing nor the maximally random jammed state[5, 6], it is worth studying the structure produced by this sequential protocol since in practical applications the packing of particles is produced by a fixed procedure such as molecular vapour deposition or dispersing particles in a solvent. In §2 we explain briefly the protocol employed. The packing of binary discs in two dimensions is studied in §3, where results of computer simulation and an analysis based on the Laguerre tessellation are given. In §4, we present results for the packing of poly-disperse discs in two dimensions and spheres in three dimensions. For the poly-disperse systems we also study the percolation process of randomly selected discs and spheres in the packed structure. Conclusion is given in §5.

2 Infinitesimal gravity protocol

In the infinitesimal gravity protocol[7], a container of $L \times L$ ($L \times L \times L$) is prepared in two (three) dimensional space. A particle (a disc in two dimensions and a sphere in three dimensions) is introduced far above the container at a horizontal position selected randomly. The radius of the particle is chosen so that the distribution of the radius R obeys a given function $\phi(R)$. Then, the particle is dropped vertically towards the bottom of the container. The particle drops freely or rolls down around a particle that it touches until the particle settles into a stable position or makes contact with the base line. (See Fig.1.) We repeat the process until the container is filled with particles. It is known that this protocol produces for a mono-disperse system a structure very close to the random close packing, though the structure is not the maximally jammed one[5, 6].

3 Binary discs

3.1 Monte Carlo simulation

Using the infinitesimal gravity protocol, we produced packed structures of two kinds of discs, one with radius R_S and the other with radius R_L . The system size is set to $L/2R_L = 100$ and discs at given fraction x of the smaller disc are packed up to a height of $140 \times 2R_L$. To reduce the effects of the boundaries, upper and lower $20 \times 2R_L$ layers are discarded (so that the remaining area is $100 \times 100 \times 4R_L^2$), and we imposed a periodic boundary condition in the horizontal direction. Then, the packing fraction f is obtained as a function of the disc size ratio $r = R_S/R_L$ and the area fraction of smaller discs $n = xR_S^2/[(1-x)R_L^2 + xR_S^2]$.

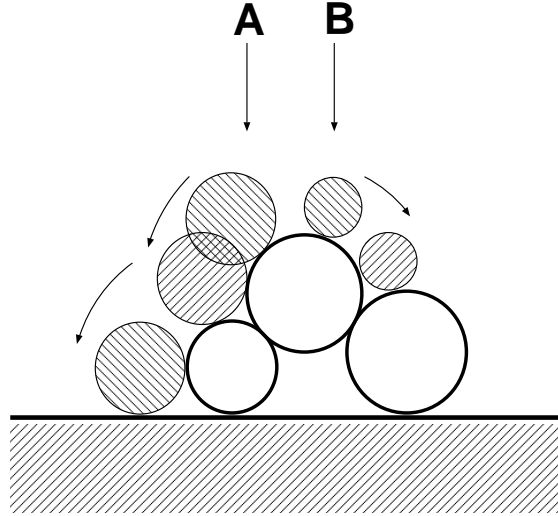


Figure 1: The infinitesimal gravity protocol is illustrated schematically. After contacting with another disc, each disc, A and B, rolls down around the target disc maintaining contact until it makes contact with another disc. It rolls down around the new disc if it can (A), and if it cannot roll down further, then it settles there (B).

The packing fractions $f(n, r)$ obtained from the Monte Carlo simulation are illustrated in Fig. 2. Note that $f(0, r) = f(1, r) = f(n, 1) = f(n, 0) = f_2 \simeq 0.82$. Here, f_2 is the packing fraction of the random close packing of monodisperse discs[8]. For $r \simeq 0$, as n is increased from $n = 0$, $f(n, r)$ increases dramatically, because of the vacant spaces between larger discs being filled by smaller discs. The increase of packing fraction reaches a maximum at a certain n where the vacant spaces are almost filled up, and decreases again to the value for the monodisperse assembly. On the other hand, $f(n, r)$ for $r \simeq 1$ decreases from f_2 as n is increased from $n = 0$, and is almost constant over the wide range of n until it increases again to f_2 near $n = 1$. The decrease of $f(n, r)$ is due to the fact that the smaller disc, which is too large to fill the vacant spaces, replaces the larger discs and destroys the structure formed by larger discs[7].

It is interesting to compare the contour for the packing fraction with the contour of the constant mean squared deviation of radii scaled by the mean diameter, $(\langle R^2 \rangle - \langle R \rangle^2)/4\langle R \rangle^2$, in the (n, r) plane, which is shown in Fig. 3. Here, $\langle R \rangle$ and $\langle R^2 \rangle$ are the mean and the mean squared radius of discs in the system, respectively. The similarity of these contours suggests that the packing fraction is determined mostly by the relative width of the distribution function. This observation is strongly supported by the results for poly-disperse systems discussed in §4.

3.2 Analysis by the Laguerre tessellation

Using the Laguerre tessellation[9], we can define adjacent neighbours of a disc and connect centres of all adjacent neighbour pairs to form a triangular network which fills the space without gaps.

For an infinite system, the mean number of adjacent neighbours for each disc is equal to 6, which is a consequence of Euler's condition, and therefore the number of

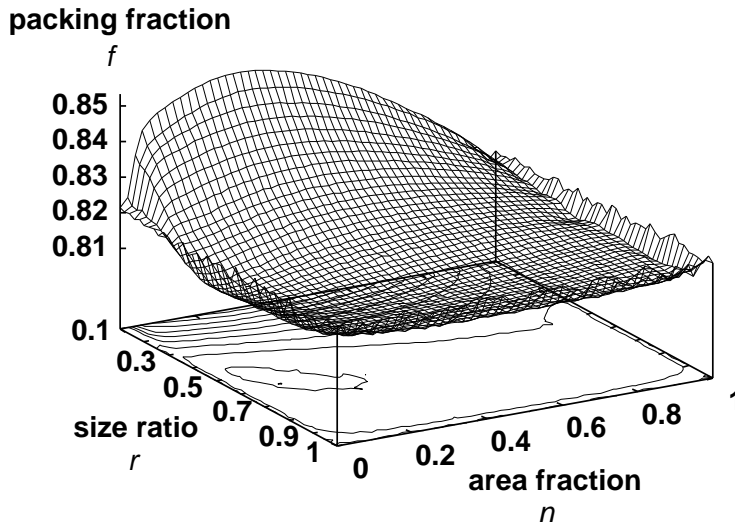


Figure 2: A 3D plot of the packing fraction f of a binary hard disc assembly as a function of size ratio r and area fraction n . Each value was determined from an average of 20 samples. The contours are drawn from 0.81 to 0.85 every 0.05.

triangles included in the system is twice as many as the number of discs. As a result, the packing fraction of the system f is expressed in term of the mean area of triangles A_m as

$$f = \frac{\pi \langle R^2 \rangle}{2A_m}. \quad (1)$$

We analysed the bond lengths in detail. The bond length distribution in our simulation is shown in Fig. 4 for the bond between two adjacent large discs. It is apparent from Fig. 4 that the major difference of bond distributions is in the behaviour of the long bond region. We can conclude that, although the tail is small compared with the whole distribution, the behaviour of the tail greatly affects the packing fraction[7].

4 Poly-disperse discs and spheres

4.1 Packing fraction

We examined the Gaussian and the uniform distributions for two and three dimensions. For two dimensions, we also examined the log-normal distribution. All distribution functions are normalized so that the average radius $\int R\phi(R)dR$ is equal to m and the mean squared deviation $\int (R - m)^2\phi(R)dR$ is equal to σ^2 . We set the average diameter $2m$ as the unit of length and use the width σ as a parameter representing the poly-dispersity.

We prepared a 200×200 ($60 \times 60 \times 60$) square (cubic) box and examined 1000 samples in two dimensions and 3000 samples in three dimensions to determined the packing fraction. In this simulation, fixed boundary conditions are imposed in horizontal directions.

Figures 5 and 6 show the dependence of f on the poly-dispersity σ . The packing fraction $f = 0.8175 \pm 0.0002$ at $\sigma = 0$ in two dimensions is consistent with the value

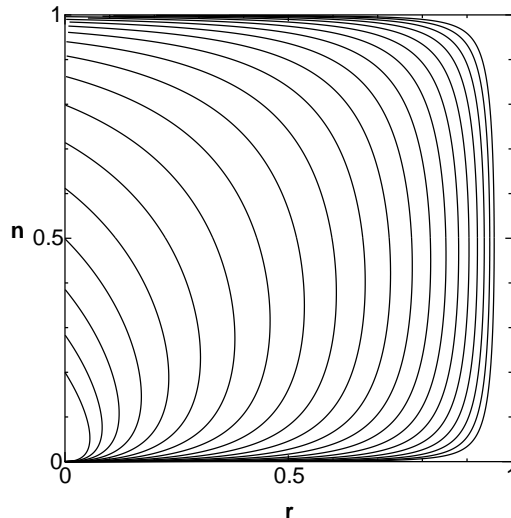


Figure 3: Contour plot of the constant mean squared deviation of radii of discs. Contours are shown for $\log \sigma = -2 \sim 0$ for every 0.1, where $\sigma \equiv \sqrt{\langle R^2 \rangle - \langle R \rangle^2} / 2\langle R \rangle$.

$f_2 = 0.82$ reported in literature[8]. Similarly, $f = 0.5575 \pm 0.0003$ at $\sigma = 0$ for three dimensions agrees well with the value $f_3 = 0.555 \pm 0.005$ reported by Onoda *et al.*[10]. When σ is increased, the packing fraction f decreases and the dependence is roughly independent of the distribution function. When σ is increased further, the packing fraction f exhibits a minimum and increases again. This behaviour is identical to the behaviour of the packing fraction of binary discs discussed in §3.

4.2 Continuum percolation

In order to construct percolation process in the random assembly of poly-disperse discs and spheres, we randomly select a given fraction of the total number of particles (coloured white at the beginning), irrespective of their size, and change their colour to black. Two black particles are regarded as connected when they touch each other. Then, we investigate the percolation of the black particles when their fraction is increased.

We determined the critical percolation area (volume) fraction A_c (V_c) of black particles as a function of σ , where percolation was judged by the appearance of a cluster spanning from the bottom to the top surface. In Figs. 7 and 8, A_c and V_c are plotted as a function of σ . Our value $A_c = 0.4777 \pm 0.0005$ and $V_c = 0.1938 \pm 0.0001$ at $\sigma = 0$ are close to the critical area fraction determined from lattice models $A_c = 0.45 \pm 0.02$ [11] and the value of $V_c = 0.185 \pm 0.005$ in literature[12].

The critical area fraction A_c is an increasing function of σ and is roughly independent of the distribution function when σ is small. In fact, if we use a power-law function

$$A_c(\sigma) = a_2 + b_2\sigma^{c_2} \quad (2)$$

to fit the data for $0 \leq \sigma \leq 0.15$, parameters are give by

$$a_2 = 0.4777 \pm 0.0005, \quad b_2 = 0.028 \pm 0.002, \quad c_2 = 0.54 \pm 0.05. \quad (3)$$

The solid line in Fig. 7 represents Eq. (2).

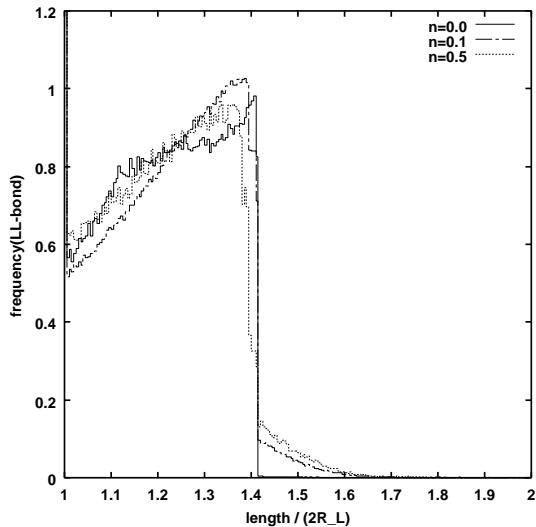


Figure 4: The distribution function of bond length between two large discs at $r = 0.9$. The solid, dash-dot and dot curves correspond to $n = 0.0$ (the mono-disperse assembly), $n = 0.1$ and $n = 0.5$. Note that each distribution function has a delta function-like peak at the length which equals $2R_L$.

The critical volume fraction V_c is a decreasing function of σ . Although the dependence is weak, this is an amazing contrast to the critical area fraction A_c in two dimensions. For $0 \leq \sigma \leq 0.15$, V_c can well be fitted by the following line

$$V_c(\sigma) = a_3 + b_3\sigma \quad (4)$$

with

$$a_3 = 0.1938 \pm 0.0001, \quad b_3 = -0.005 \pm 0.001, \quad (5)$$

which is shown by the solid line in Fig. 8.

The significant difference in the poly-dispersity dependence of the critical area and volume fractions can be explained by the surface area of discs and spheres which determines the effectiveness of connection[13]. In fact, we can easily show that while the average circumference of discs is independent of σ , the average surface area of spheres increases as σ is increased.

5 Concluding remarks

We have examined by Monte Carlo simulation the packing fraction of poly-disperse discs and spheres which are packed in two and three dimensions by the infinitesimal gravity protocol. It is a striking result that the packing fraction decreases for the weak poly-dispersity. This is due to the fact that a little increase of poly-dispersity makes particles hard to adjust vacant spaces and further increase of σ introduces smaller particles filling up vacant spaces. It is an open and interesting mathematical question if one can rigorously prove this effect in general.

We have also studied the continuum percolation of poly-disperse systems in two and three dimensions and have shown that the critical area fraction in two dimensions and

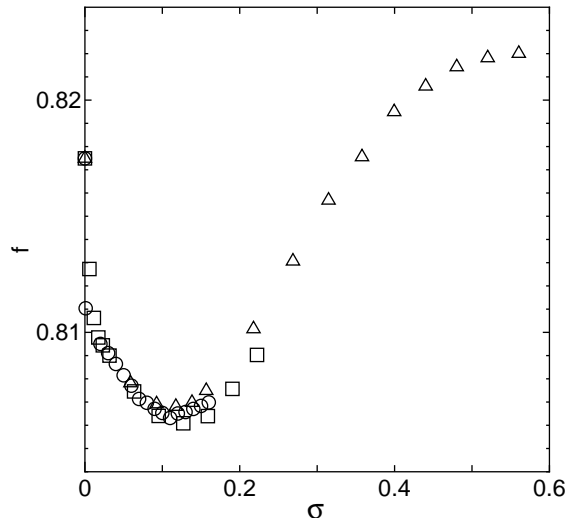


Figure 5: The relation between f and σ for various size distribution functions in two dimensions: The results are shown for Gaussian (circles), uniform (squares), and log-normal (triangles) distributions.

the critical volume fraction in three dimensions have opposite dependence on the polydispersity. Furthermore, the critical area (volume) fraction is shown not to depend much on the distribution function. These results indicate that the concept of the critical area (volume) fraction as a dimensional invariant[11] has to be applied with some caution.

This work was supported in part by the grant from the Ministry of Education, Science, Sports and Culture.

References

- [1] J. D. Bernal, *Nature* **183**, 141 (1959).
- [2] B. J. Alder and T. E. Wainwright, *J. Chem. Phys.* **27**, 208 (1957).
- [3] H. M. Jaeger and S. R. Nagel, *Science* **255**, 1523 (1992).
- [4] R. Katoh, T. Hihara, D. L. Peng and K. Sumiyama, *Appl. Phys. Lett.* **82**, 2688 (2003).
- [5] S. Torquato, T. M. Truskett and P. G. Debenedetti, *Phys. Rev. Lett.* **84**, 2064 (2000).
- [6] T. M. Truskett, S. Torquato and P.G. Debenedetti, *Phys. Rev. E* **62**, 993 (2000).
- [7] T. Okubo and T. Odagaki, *J. Phys.: Condens. Matter* **16**, 6651 (2004).
- [8] J. G. Berryman, *Phys. Rev. A* **27**, 1053 (1982).

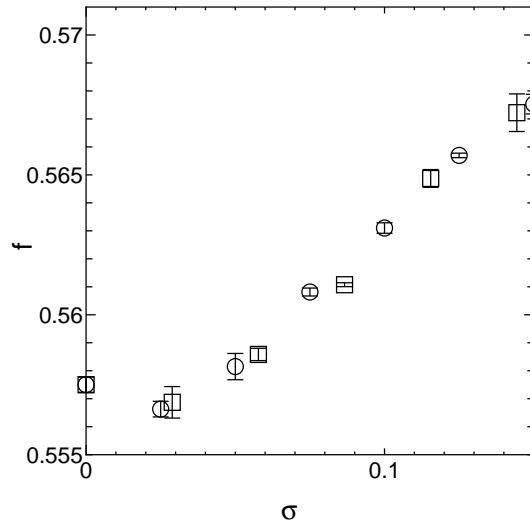


Figure 6: The relation between f and σ for two size distribution functions in three dimensions: The results are shown for Gaussian (circles) and uniform (squares) distributions.

- [9] B. J. Gellatly and J. L. Finney, *J. Non-Cryst. Solids* **50**, 313 (1981).
- [10] G. Y. Onoda and E. G. Liniger, *Phys. Rev. Lett.* **22**, 2727 (1990).
- [11] H. Scher and R. Zallen, *J. Chem. Phys.* **53**, 1421 (1970).
- [12] D. Bouvard and F. F. Lange, *Acta metall. mater.* **39**, 3083 (1991).
- [13] R. Ogata, T. Odagaki and K. Okazaki, *J. Phys.: Condens. Matter* **17**, 4531 (2005).

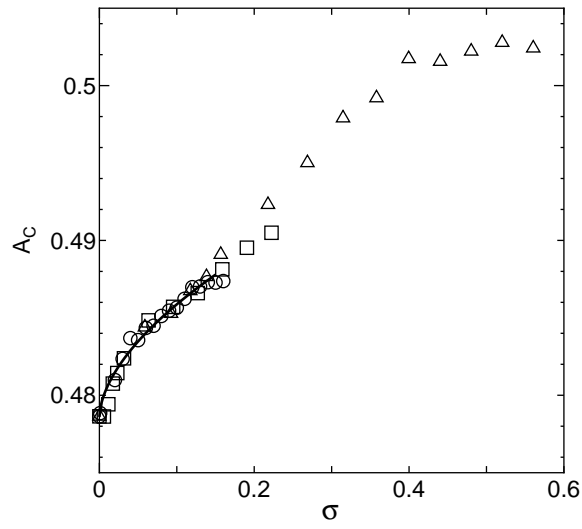


Figure 7: The critical area fraction A_c is plotted against σ for three size distribution functions: Gaussian (circles), uniform (squares) and log-normal (triangles). The solid line represents the fitting function (2). Error bars are much smaller than the size of the symbols.

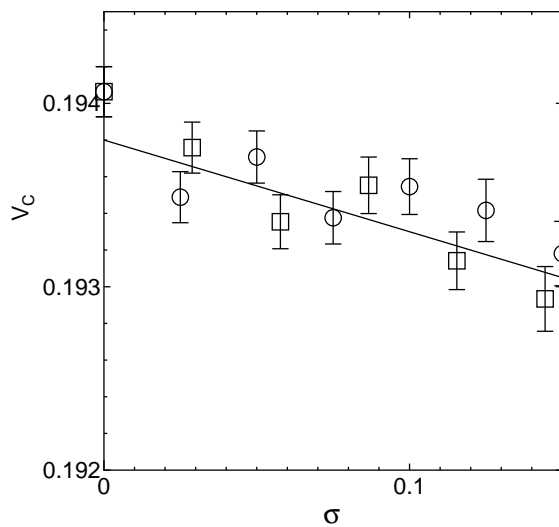


Figure 8: The critical volume fraction V_c is plotted against σ for two size distribution functions: Gaussian (circles) and uniform (squares). The solid line represents function (4).